Temperature measurements in Xe+Cu at 30 MeV/nucleon: Size effects in the caloric curve

P. M. Milazzo, G. Vannini, D. Fontana, G. V. Margagliotti, P. F. Mastinu, R. Rui, and F. Tonetto
Dipartimento di Fisica and INFN, Trieste, Italy

N. Colonna
INFN, Bari, Italy

A. Botvina,* M. Bruno, M. D'Agostino, and M. L. Fiandri
Dipartimento di Fisica and INFN, Bologna, Italy

F. Gramegna
INFN, Laboratori Nazionali di Legnaro, Italy

A. Moroni
Dipartimento di Fisica and INFN, Milano, Italy

(Received 22 December 1998; published 30 August 1999)

Results of experiments performed to investigate the Xe+Cu 30 MeV/nucleon reaction are presented. The decay products coming from the disassembly of the unique source formed in central collisions and those coming from the decay of the quasiprojectile in peripheral and midperipheral ones have been identified through a careful data selection taking into account the experimental efficiency distortion on energy and angular distributions. The nuclear temperatures of these decaying systems have been measured from the relative isotopic abundances; the excitation energies of the fragment sources have been extracted by means of model calculations. The results have been compared to those obtained in the study of the Au+Au 35 MeV/nucleon in order to probe the effects of the finite size of the intermediate mass fragment emitting source on the relationship between its excitation energy and temperature. The studied fragment emitting sources have mass $A_1 \simeq 130$, $A_2 \simeq 200$, $A_3 \simeq 300$; moreover, the A_2 system have been investigated via two different reaction channels: the quasiprojectile of peripheral Au+Au and the unique fused system of the Xe+Cu central collisions. The relationship between temperature and excitation energy seems to be almost independent on the size of the emitting source and on the reaction entrance channel. On the contrary a weak dependence arises when individual thermometers are considered. [S0556-2813(99)03009-5]

PACS number(s): 21.65.+f, 25.70.Pq, 64.30.+t

I. INTRODUCTION

In heavy ion reactions at intermediate energies different decaying systems are formed depending on the impact parameter. The deexcitation of these systems takes place through the emission of fragments (light, intermediate, and heavy mass fragments), i.e., they behave as fragment sources which differ in size, shape, excitation energy, and even the way in which they are formed. In particular for excitation energies above 2 MeV/nucleon multifragmentation takes place as one of the possible deexcitation process.

One of the main goals of multifragmentation studies is to map the nuclear phase diagram. In fact the particular form of the nuclear forces leads, for infinite nuclear matter, to an equation of state similar to that of the Van der Waals gas, which is likewise characterized by the existence of a liquid-gas phase transition [1]. For finite nuclear systems the situation is more complicated; however, from the theoretical point of view, microscopic statistical models predict the existence of a phase transition at excitation energies where nuclear systems undergo multifragment decays [2,3] and several experiments [4–6,8] showed the existence of signals related to a possible liquid-gas phase transition. Some experimental signals rely on the particular shape of the caloric curve. If some results [4] agree with predictions of statistical multifragmentation models [3] and are reminiscent of a (first order) phase transition, other experimental data suggest that multifragmentation may result from a continuous phase transition near the critical point [5,6]. The main difference in the case of Au fragmentation [4,6,7] lies on the presence or absence of a plateau of nearly constant temperature (4.5–5.5 MeV) for excitation energies ranging from about 4 to 8 MeV/nucleon, followed by a steep rise at higher excitation energies. For lighter systems [9] the observed trend of the caloric curve is a monotonic increase up to excitation energies of some tens of MeV/nucleon.

In this paper we investigate in detail the region of excitation energy 4–6 MeV/nucleon of the caloric curve. We present the results of temperature measurements for central and peripheral Xe+Cu 30 MeV/nucleon. By comparing these results with those obtained for the Au+Au 35 MeV/nucleon [7] (2–6 MeV/nucleon excitation energy) we also

*On leave from the Institute for Nuclear Research, Ru-117312 Moscow, Russia.

investigate size effects and entrance channel dependence of the caloric curve of finite and equilibrated systems.

In Sec. II a brief description of the experimental conditions is given. Section III describes the data analysis devoted to the identification and characterization of emitting sources. In Sec. IV the experimental results, regarding the temperature and excitation energy investigation, are presented and discussed, then the conclusions are drawn in Sec. V.

II. EXPERIMENTAL METHOD

In order to investigate the reactions Xe+Cu at 30 MeV/nucleon and Au+Au at 35 MeV/nucleon experiments were performed at the National Superconducting K1200 Cyclotron Laboratory of the Michigan State University. The angular range $3° < \theta_{lab} < 23°$ was covered by the MULTICS array [10]. The identification thresholds in the MULTICS array were about 1.5 MeV/nucleon for charge identification and about 10 MeV/nucleon for mass identification. The MULTICS array consisted of 48 telescopes, each of which was composed of an ionization chamber (IC), a silicon position-sensitive detector (Si), and a CsI crystal. Typical energy resolutions were 2, 1, and 5% for IC, Si and CsI, respectively. Light charged particles and fragments with charge up to $Z=20$ were detected at $23° < \theta_{lab} < 160°$ by the phoswich detectors of the MSU Miniball hodoscope [11]. The charge identification thresholds were about 2, 3, 4 MeV/nucleon in the Miniball for $Z=3$, 10, 18, respectively. In the Xe+Cu 30 MeV/nucleon reaction the $3° < \theta_{lab} < 8°$ angular range was covered by a mask to avoid radiation damage of silicon detectors. However the geometric acceptance of the combined array was greater than 87% of 4π.

The multiplicity of detected charged particles (Nc) was used for impact parameter b reconstruction [12]:

$$\hat{b} = b/b_{max} = \left(\int_{Nc}^{+\infty} P(N'c)\, dN'c \right)^{1/2}.$$

Here $P(Nc)$ is the charged particle probability distribution and $\pi \cdot b_{max}^2$ is the measured reaction cross section for $Nc \geqslant 3$.

III. IDENTIFICATION OF THE FRAGMENT EMISSION SOURCES

To gain more insight into the characteristics of the caloric curve of finite nuclear systems and the possible existence of a phase transition, one must measure the temperatures of well defined and experimentally identified systems, with different excitation energy and size, using reliable thermometers. Indeed to calculate the temperature through double ratios of isotope yields, following the prescriptions of Ref. [13] one should have to verify that (i) free nucleons and composite fragments are contained within a certain volume V at a single temperature T and are in thermal equilibrium, (ii) it is possible to use the Maxwell-Boltzmann statistics, (iii) the system has reached the chemical equilibrium, (iv) the experimental yield of a fragment is proportional to its density inside the volume V, (v) all detected nuclei originate from a single source. The double ratio R of the yields Y of four isotopes in their ground states, prior to secondary decay is then given by

$$R = \frac{Y(A_1,Z_1)/Y(A_1+1,Z_1)}{Y(A_2,Z_2)/Y(A_2+1,Z_2)} = \frac{e^{B/T}}{a}, \qquad (1)$$

where a is a constant related to spin and mass values and

$$B = BE(Z_1,A_1) - BE(Z_1,A_1+1) - BE(Z_2,A_2) + BE(Z_2,A_2+1),$$

and $BE(Z,A)$ is the binding energy of a nucleus with charge Z and mass A [13].

In principle, the temperature dependence of the isotope ratio R allows for determination of the temperature T. However, primary fragments can be highly excited [14] so that secondary decays from higher lying states of the same and heavier nuclei can lead to non-negligible distortions to the measured ratios R, that need to be corrected [15] to recover information on early temperature. To reduce the sensitivity to such corrections, it is advisable to choose cases for which $B \gg T$ since the uncertainties on T are proportional to T/B.

Since, however, not all the prescriptions related to the double ratios method [13] are experimentally accessible, it is worthwhile to apply to the data a procedure which allows us to identify the emitting systems and to verify that all the isotopes, used for the temperature determination, come from the same source. For this purpose in our analysis, for each selected impact parameter range, we verify that all the detected decay products are emitted nearly isotropically from the same source and that their energy distribution have Maxwellian shapes, i.e., that angular and energy distributions are compatible with a statistical emission providing an experimental indication of reached thermalization.

A difficulty in assessing isotropic emission comes from the fact that isotopic resolution was only obtained over a limited angular range (MULTICS array). Angular distributions and energy are thus distorted by the acceptance of the apparatus. To evaluate these distortions, a fragment source isotropically emitting in its c.m. frame was simulated and the calculated angular and energy distributions of its products were filtered by the acceptance of the apparatus. This full consistent method was used and results already published in the analysis of the Au+Au 35 MeV/nucleon [7].

In the following we only describe the prescriptions applied to the Xe+Cu 30 MeV/nucleon experimental data, before analyzing them in terms of temperatures. For central collisions the velocity of the unique isotropically emitting source has been chosen as that of the center of mass in the laboratory frame (5.1 cm/ns). On the contrary, when looking at peripheral collisions, different velocities of the quasiprojectile (QP) source yield different angular and energy experimental distributions in the c.m. of the QP; therefore a best fit to the experimental distribution of all isotopes from H to C was used to extract the velocity of the QP emitting source (v_{QP}) for each bin of impact parameter (see the second column of Table II). As it may be expected, v_{QP} decreases going from peripheral towards midperipheral colli-

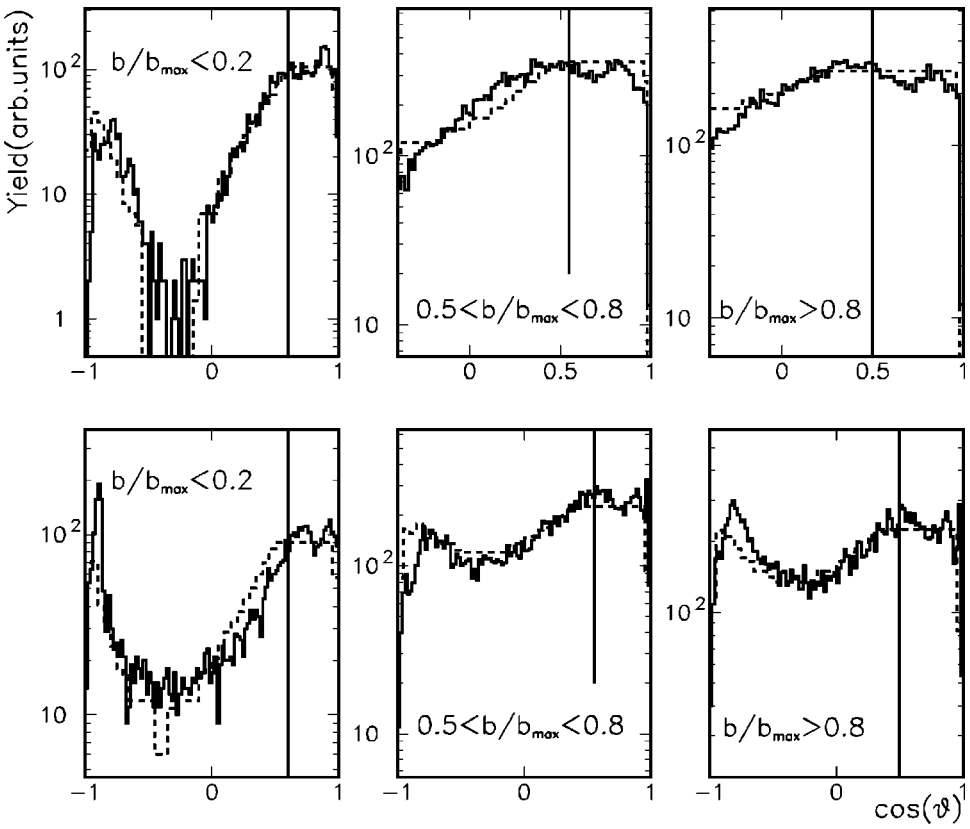

FIG. 1. Angular distributions for Carbon isotopes (upper panels) and ^{6}He (lower panels) for the three impact parameter region investigated. Full line: experimental data, dashed line: simulation (see text). The vertical lines show the angular range chosen for the temperature analysis.

sions. This decrease in QP velocity is directly related to an increase on excitation energy of the emitting QP source. It should be noted that a unique v_{QP} for each selected impact parameter reproduces the experimental angular distribution of each isotope.

Simulations indicate that distortions in the angular distribution, due to detection inefficiencies, are negligible in the range up to 60°, 55° and 45° in the reference frame of the emitting source for QP peripheral, QP midperipheral and unique central source. Figure 1 gives an example of the experimental (full lines) and simulated (dashed lines) angular distribution for the three cases and for different fragments. Some discrepancies between experimental and simulated distributions appear in the backward angle region (in the analysis only data at the right side of the vertical lines are considered) due to the fact that the simulation does not take into account in detail the inefficiencies introduced by dead surfaces on the array (i.e., detectors frames) or difference in the energy threshold for mass identification (the silicon detectors have different thickness, from 480 to 520 μm).

To further check the equilibration of the emitting source for the data selected with angular cuts we looked at the energy distributions of the emitted isotopes. The distributions have Maxwellian shapes with similar slopes for all the isotopes. In Fig. 2 the energy distribution of three isotopes is presented together with the curves obtained by fitting the data with pure Maxwellian functions. The obtained T_{Maxw} values are similar within the errors for all isotopes (in Table II are reported the average values). This holds for all cuts on impact parameter considered. This behavior gives further indications that the necessary condition of equilibration of the fragmenting systems is satisfied.

The obtained values for the parameter related to the apparent temperature T_{Maxw} (see Table II) are higher than those extracted from isotope ratios. Several experimental studies showed temperature values obtained from Maxwellian fits higher than that extracted from isotope ratios or level population ratios [16]; moreover the T_{Maxw} values are even higher than typical temperatures used in statistical models to repro-

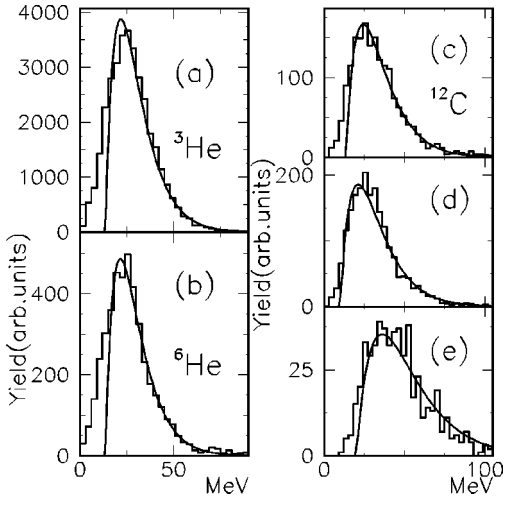

FIG. 2. Energy distribution and Maxwellian fit for different isotopes in peripheral [(a)–(c), $\hat{b}>0.8$], midperipheral [(d), $0.5<\hat{b}<0.8$], and central collisions (e). The obtained values for the parameter related to the apparent temperature T_{Maxw} are 8.3±0.5 (a), 8.1±0.5 (b), 10.6±0.7 (c), 12.1±0.8 (d), 16.±1.2 (e), respectively.

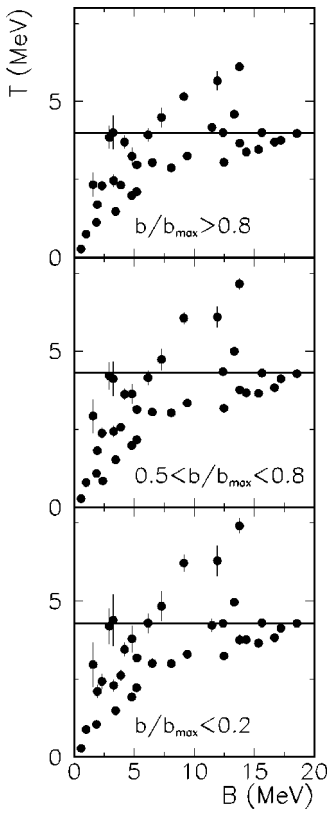

FIG. 3. Temperature extracted from different isotope thermometers as a function of the *B* parameter [13]; the full line suggests the asymptotic value T_{iso} of the isotope temperature.

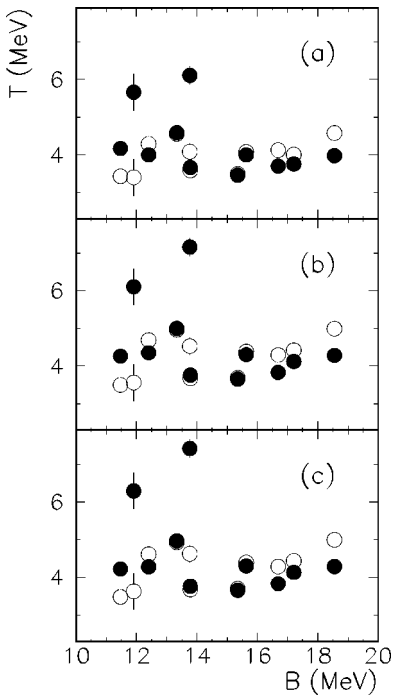

FIG. 4. Temperature extracted from the ''best'' isotope thermometers as a function of the *B* parameter [13], from experimental data (solid circles) and after correction for sequential decay feeding [15,19] (open points) [(a) Peripheral collisions, (b) midperipheral, (c) central].

duce the experimental spectra [2,3]. A tentative explanation of this difference has been done in the framework of standard statistical models [9]. In particular one has to take into account the Fermi motion of nucleons [17] and variations in the Coulomb barrier depending on the point of emission within the system; one has also to recall that the T_{Maxw} values are averaged over the deexcitation chain and are also affected by successive recoil effects.

IV. TEMPERATURE MEASUREMENTS AND DEDUCED EXCITATION ENERGY

In the previous section we have shown that the results on the angular and energy analysis confirm that the conditions of the identification and equilibration of the isotope source seem to be satisfied. The isotope ratios method can be therefore applied to calculate the temperature of the emitting sources. Taking the set of data coming from a single source selected by means of the angular and charged particle multiplicity cuts above described, the good isotopic resolution of the apparatus (up to carbon) allows the extraction of temperatures from a high number of isotope ratios (41).

Figure 3 shows isotope-ratio temperatures as a function of the parameter B [see Eq. (1)]. The best thermometers are those that deal with yields of isotopes with large difference in the ground state binding energies — in fact for large *B* values we observe that the extracted temperatures tend towards an asymptotic value — the average values of the temperature extracted from the highest *B* values thermometers T_{iso} are 4.0, 4.3, and 4.3 MeV for QP peripheral, QP midperipheral, and unique central source, respectively. Figure 4 and Table I give the values for 11 thermometers with $B>9$ MeV (full circles).

The fluctuations in the temperature obtained from different thermometers are likely due to secondary decays of highly excited fragments. As explained in Ref. [18] it is possible to use sequential decay calculations, to evaluate the modification to the initial distributions due to the particle whose decay feeds the measured yields. In Refs. [15,19] an empirical procedure was proposed, to strongly reduce these fluctuations. It was also shown [15] that for temperatures in the neighborhood of 4 MeV these empirical correction factors do not depend either on the size or on the N/Z ratio of the decaying systems. The experimental temperatures of the present measurement, corrected as suggested in Ref. [15] are plotted in Fig. 4 (open circles) and reported in Table I. The 11 thermometers used suggest a break-up temperature T_0, defined as the mean value of the corrected temperatures, of the nuclear decaying system of 3.9, 4.2, and 4.2 MeV for QP peripheral, QP midperipheral, and unique central source, respectively. These values are slightly different from that published in Ref. [19] because of the different data selection; in the present study only the part of the angular distribution consistent with a thermalized source is taken into account for the analysis. Since the aim of this paper is the identification of well defined emitting sources and the study of their thermalization we needed a refined and careful data selection.

Before we come to any conclusions on temperature mea-

TABLE I. Temperatures extracted from different double yield isotope ratio (T_{exp}) and calculated values after sequential feeding correction (T_{corr}).

	$\hat{b}$	T_{exp} (MeV)	T_{corr} (MeV)
^{3}He/^{4}He−^{6}Li/^{7}Li	>0.8	4.59±0.04	4.56±0.04
^{3}He/^{4}He−^{7}Li/^{8}Li	>0.8	3.98±0.03	4.58±0.03
^{3}He/^{4}He−^{9}Be/^{10}Be	>0.8	6.11±0.13	4.08±0.09
^{3}He/^{4}He−^{11}B/^{12}B	>0.8	3.76±0.06	4.01±0.06
^{3}He/^{4}He−^{12}C/^{13}C	>0.8	4.00±0.06	4.08±0.06
^{3}He/^{4}He−^{13}C/^{14}C	>0.8	4.00±0.09	4.29±0.10
^{6}Li/^{7}Li−^{11}C/^{12}C	>0.8	4.17±0.14	3.44±0.12
^{7}Li/^{8}Li−^{11}C/^{12}C	>0.8	3.70±0.08	4.13±0.09
^{9}Be/^{10}Be−^{11}C/^{12}C	>0.8	5.66±0.30	3.41±0.18
^{11}B/^{12}B−^{11}C/^{12}C	>0.8	3.47±0.11	3.50±0.11
^{11}C/^{12}C−^{12}C/^{13}C	>0.8	3.67±0.12	3.59±0.12
^{3}He/^{4}He−^{6}Li/^{7}Li	0.5–0.8	5.00±0.05	4.96±0.05
^{3}He/^{4}He−^{7}Li/^{8}Li	0.5–0.8	4.29±0.03	4.99±0.03
^{3}He/^{4}He−^{9}Be/^{10}Be	0.5–0.8	7.16±0.17	4.53±0.11
^{3}He/^{4}He−^{11}B/^{12}B	0.5–0.8	4.12±0.06	4.43±0.06
^{3}He/^{4}He−^{12}C/^{13}C	0.5–0.8	4.30±0.07	4.39±0.07
^{3}He/^{4}He−^{13}C/^{14}C	0.5–0.8	4.35±0.10	4.69±0.11
^{6}Li/^{7}Li−^{11}C/^{12}C	0.5–0.8	4.26±0.14	3.50±0.12
^{7}Li/^{8}Li−^{11}C/^{12}C	0.5–0.8	3.83±0.08	4.29±0.09
^{9}Be/^{10}Be−^{11}C/^{12}C	0.5–0.8	6.10±0.34	3.56±0.20
^{11}B/^{12}B−^{11}C/^{12}C	0.5–0.8	3.65±0.11	3.69±0.11
^{11}C/^{12}C−^{12}C/^{13}C	0.5–0.8	3.76±0.12	3.68±0.12
^{3}He/^{4}He−^{6}Li/^{7}Li	<0.2	4.97±0.07	4.93±0.07
^{3}He/^{4}He−^{7}Li/^{8}Li	<0.2	4.29±0.04	5.00±0.05
^{3}He/^{4}He−^{9}Be/^{10}Be	<0.2	7.41±0.24	4.63±0.15
^{3}He/^{4}He−^{11}B/^{12}B	<0.2	4.13±0.08	4.44±0.09
^{3}He/^{4}He−^{12}C/^{13}C	<0.2	4.30±0.09	4.39±0.09
^{3}He/^{4}He−^{13}C/^{14}C	<0.2	4.28±0.13	4.61±0.14
^{6}Li/^{7}Li−^{11}C/^{12}C	<0.2	4.22±0.20	3.48±0.16
^{7}Li/^{8}Li−^{11}C/^{12}C	<0.2	3.83±0.12	4.29±0.13
^{9}Be/^{10}Be−^{11}C/^{12}C	<0.2	6.29±0.49	3.62±0.29
^{11}B/^{12}B−^{11}C/^{12}C	<0.2	3.66±0.14	3.70±0.14
^{11}C/^{12}C−^{12}C/^{13}C	<0.2	3.76±0.17	3.68±0.17

surement we have to recall that the isotope temperature can result from an average upon the time-scale for source disintegration [20]. In fact if the system deexcites by sequentially emitting, theoretical predictions [21,22] indicate that different isotope can be preferentially produced in different step of the disintegration chain. The observation of a non-negligible decay time scale, however, does not necessarily imply a failure of simultaneous decay models if the decay time is shorter than the equilibration time [23]. In previous studies on the Xe+Cu 30 MeV/nucleon reaction [24] the three-body Coulomb trajectory calculations showed a mean emission time of $\approx$200 fm/c, consistent with a fast sequential decay. In the same spirit the double ratio method can operate an average of the temperature over the isotope emission time.

In order to investigate the caloric curve of the finite nuclear matter we need to extract information also on the excitation energy values of the decaying studied systems. Starting from the v_{QP} values obtained we can fix an upper limit to the excitation energy (E_v^*) of the source in a simple way using momentum conservation and assuming that the excitation energy is shared between projectile and target in proportion to their mass (Table II):

$$E_v^* = \frac{m_{Xe}}{(m_{Xe}+m_{Cu})}\left(\frac{1}{2}m_{Xe}(v_P^2 - v_{QP}^2) - \frac{1}{2}\frac{m_{Xe}^2}{m_{Cu}}(v_P - v_{QP})^2\right), \quad (2)$$

where v_{QP} and v_P are the QP and projectile velocity in the laboratory frame. In this way we completely neglect preequilibrium emission and mass and excitation energy transferred to a neck or fireball system, if formed. Since for the considered system sizes and incident energy nonequilibrated fragment emissions are present [25] the expected excitation energy must have lower values than the E_v^* ones.

Excitation energies were also estimated assuming the equilibration of the emitting systems and comparing the data with the microcanonical statistical multifragmentation model (SMM) [3] to describe the experimental findings of the fragment emission. The statistical model SMM was used to investigate the decay of the QP peripheral, QP midperipheral, and central unique source by looking at the excitation energy ranges able to reproduce the measured charge distribution. In the peripheral and midperipheral cases the calculations were made for a Xe nucleus, while a charge $Z=71$, as suggested by systematics studies on incomplete fusion [26], was used as input for the central source. In all the three cases one third of the normal density was fixed and excitation energies ranging from 0 to 8 MeV/nucleon were considered.

The velocity of the fragment source was assumed as in the experimental case. The events generated by SMM for different input excitation energies were filtered by the apparatus. Each experimental charge distribution was reproduced by properly choosing SMM excitation energy intervals. It was found that the minimum value of the excitation energy is fixed by the reproduction of the high tail of the charge distribution, while the upper value is fixed by the reproduction of the yield of light fragments. In Fig. 5 the experimental

TABLE II. Emitting source characteristics for each bin of impact parameter.

$\hat{b}$	v_{source} (cm/ns)	E_v^*/A (MeV/nucleon)	E_{SMM}^* (MeV/nucleon)	T_{Maxw} (MeV)	T_{iso} (MeV)	T_0
>0.8	6.3±0.1	5.1	4.0±0.5	9.0±2.0	4.0	3.9±0.4
0.5–0.8	6.0±0.1	5.7	5.0±0.5	11.0±2.0	4.3	4.2±0.5
<0.2	5.1±0.1		5.5±0.5	15.0±3.0	4.3	4.2±0.5

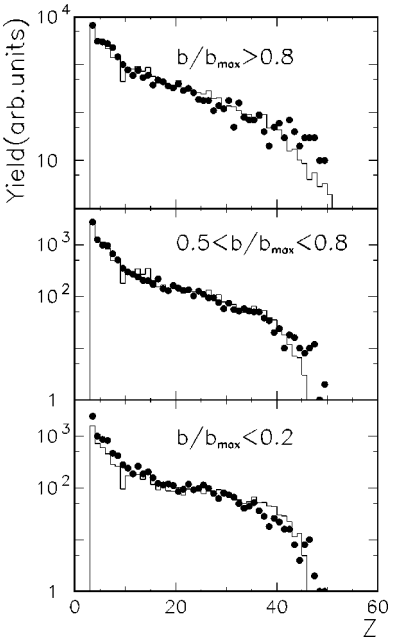

FIG. 5. Charge distributions (solid points: experimental data, full line: SMM predictions).

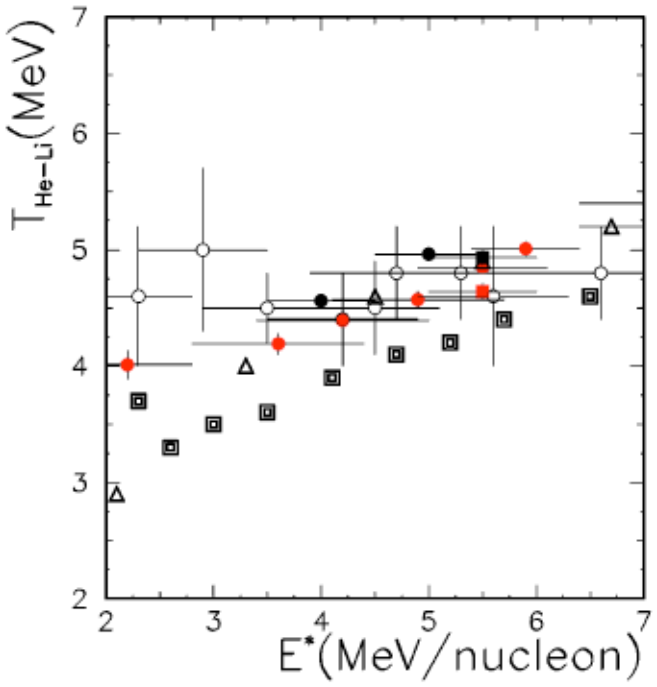

FIG. 6. (Color) Experimental caloric curve: open points, Ref. [4]; double squared open symbols, Ref. [6]; open triangles, Ref. [9]; full points, present data (red Au+Au, black Xe+Cu; the full squares refer to central collisions).

charge distributions and the corresponding SMM predictions are shown for the three impact parameter intervals. It is worthwhile to stress that for peripheral collisions the range in which it is possible to choose the source size is strictly limited by the value of the highest observed charges. Moreover to evaluate the sensibility of the extracted excitation energies to the value of the source density and size the procedure has been repeated for different density values (1/6–1/2 ρ_0) and system charge (80–90 % of the total charge for central collisions) finding differences of the order of 0.5 MeV/nucleon in the extracted excitation energy values. In fact charge distributions appear to be more sensitive to excitation energy than to the other SMM input parameters [27].

In Table II the excitation energy ranges used to get agreement between SMM predictions and experimental data are summarized. For this experiment it was not possible to perform an evaluation of the excitation energy through calorimetry since in a large fraction of events the largest fragment was not detected because of the mask covering angles lower than 8°. We want to stress that in previous applications [7] within the uncertainties of the two procedures a good agreement between the values predicted by SMM and those obtained with the calorimetric method was found.

In order to have a comparison with other published results in Fig. 6 the temperatures obtained with the ^{6}Li/^{7}Li-^{3}He/^{4}He thermometer (T_{HeLi}) are plotted as a function of the excitation energy for which SMM predictions match the experimental charge distributions (solid points, black for Xe+Cu, red Au+Au, circles for peripheral, squares for central collisions). They show a slow, continuous increase with excitation energy. The shape of the obtained caloric curve agrees with previous results of the EOS Collaboration [6] (double squared points) and with studies on the fragmentation of lighter projectiles (open triangles) [9].

One should note that the fused system in central Xe+Cu collision has charge and mass characteristics similar to an Au nucleus. Therefore we can compare the QP formed in Au+Au peripheral collisions with the source formed in central Xe+Cu reactions. In particular we note that both these systems show within the experimental errors the same temperature at the same excitation energy (about 5.5 MeV/nucleon). Since the same system was formed starting from different entrance channel for the reaction this is an indication that thermodynamical equilibrium was achieved before the deexcitation.

The presented data are coming from systems different in size, from a mass 129 for the QP of the Xe+Cu collisions up to more than 300 nucleons of the central Au+Au ones. We wish to point out that care must to be taken before drawing conclusions based on the observation of a single isotope thermometer (i.e., ^{6}Li/^{7}Li-^{3}He/^{4}He). In Fig. 7 we plot the temperatures obtained with the ^{6}Li/^{7}Li-^{3}He/^{4}He (T_{HeLi}) and the ^{12}C/^{13}C-^{11}C/^{12}C (T_{C}) thermometers as a function of the excitation energy; open points correspond to Xe+Cu data, solid points are for the Au+Au reaction. We observe that using different isotope thermometers one could get conflicting results; looking, for instance, at the T_{HeLi} one gets a slow increasing behavior with excitation energy (and it would be possible to infer on a second order phase transition of the nuclear matter); on the contrary the T_{C} thermometer shows a flat caloric curve (from which one could suggest a first order phase transition). Moreover even if the behavior of the caloric curve is similar for the two measured reactions, one has to note that the values of the temperatures are slightly different. This is due to the N/Z ratio of the different emitting systems, that directly implies on the probability of produc-

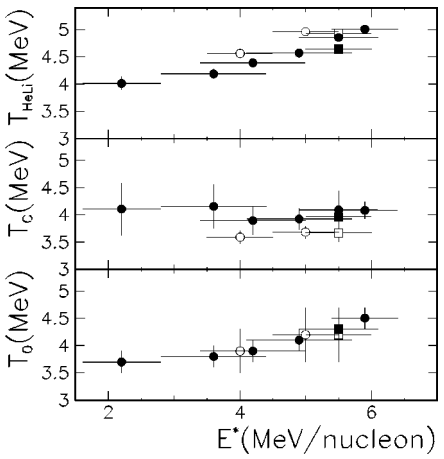

FIG. 7. T_{Heli}, T_{C} (see text) and the corrected temperature T_0 as a function of the excitation energy. Open symbols Xe+Cu reaction (present work), full symbols Au+Au [7]; squares indicate central collisions.

tion of neutron-poor fragments (as in the ^{11}C case). In order to avoid this kind of problem we believe that using a full set of reliable thermometers override the effect of size and N/Z ratio of the emitting source on each single isotope double ratio, since a more detailed dependence of temperature from the excitation energy can be investigated. In this respect, looking at the lowest panel of Fig. 7, where the extracted corrected T_0 temperatures are plotted for the different analyzed systems, it is possible to conclude that, within the experimental errors, the caloric curve does not seem to be affected significantly from the mass of the emitting system.

We should note that the procedure used for the corrections of the isotope temperature is not unique, e.g., even if SMM calculations reasonably reproduce the behavior of the caloric curve extracted from isotope thermometers, however, this model gives values approximately 1–1.5 MeV higher for the freeze-out temperatures [7]. On the other hand, the predictions of SMM on the excitation energies are directly related to the charge distributions and, then, in the thermalization assumption, represent a reliable evaluation. Moreover, when a comparison with excitation energy measurement was possible, a good agreement with SMM predictions was found [7].

V. CONCLUSION

In the study of the Xe+Cu 30 MeV/nucleon and Au+Au 35 MeV/nucleon reactions it was possible to investigate the characteristics of different types of emitting sources: the unique one formed in central collisions and the quasiprojectile sources at different excitation energies in peripheral ones. The studied fragment emitting sources have mass ranging from 129 up to more than 300 nucleons. The same system, Au-like, has been investigated via two different reaction channel comparing the peripheral Au+Au collisions with the Xe+Cu central ones.

All these sources emit several light and intermediate mass fragments. A careful data selection was devoted to isolate single emitting sources. The experimental angular distributions of the fragments and model calculations indicate that these sources may have reached a thermal equilibrium. We measured the temperatures of these emitting systems with a high number (41) of isotopes ratios. The best thermometers are those with a high value of the B parameter of Eq. (1), therefore we used only those with $B>9$ MeV. In this way we had 11 measurements of the temperature for each nuclear system, 5 of which do not use the ^{3}He/^{4}He ratio, but involve heavier isotopes for which the problem of pre-equilibrium contamination is expected to be less important. The values of these temperatures have been corrected empirically for secondary decays and a very good agreement has been found for all the 11 corrected temperatures.

We also compared the experimental charge distributions with the predictions of the SMM model to get information on the excitation energy of the emitting sources. In order to investigate the trend of the caloric curve we have used a large set of isotope thermometers. Even if some single thermometers reveal a dependence on the size and N/Z of the emitting system, their average is almost insensitive to the entrance channel. Therefore we conclude that the observed trend of the global caloric curve, both for the reactions Xe+Cu 30 MeV/nucleon and Au+Au 35 MeV/nucleon, shows a monotonic increase with the excitation energy. In summary we showed that in order to investigate the caloric curve it is advisable to deal with a full set of reliable thermometers.

ACKNOWLEDGMENTS

The authors are indebted to R. Bassini, C. Boiano, S. Brambilla, G. Busacchi, A. Cortesi, and M. Malatesta for their skillful assistance. This work was supported in part by grants of the Italian Ministry of University and Scientific and Technological Research (MURST).

[1] U. Mosel *et al.*, Nucl. Phys. **A236**, 252 (1974); G. Sauer *et al.*, *ibid.* **A264**, 221 (1976); H. R. Jaqaman *et al.*, Phys. Rev. C **27**, 2782 (1983); **29**, 2067 (1984).

[2] D. H. Gross, Phys. Rev. Lett. **56**, 1544 (1986); Rep. Prog. Phys. **53**, 605 (1990); Phys. Rep. **257**, 133 (1995).

[3] J. P. Bondorf *et al.*, Nucl. Phys. **A444**, 460 (1986); A. S. Botvina *et al.*, *ibid.* **A475**, 663 (1987); J. P. Bondorf *et al.*, Phys. Rep. **257**, 133 (1995).

[4] J. Pochodzalla *et al.*, Phys. Rev. Lett. **75**, 1040 (1995).

[5] J. B. Elliot *et al.*, Phys. Rev. C **49**, 3185 (1994); M. L. Gilkes *et al.*, Phys. Rev. Lett. **73**, 1590 (1994).

[6] J. A. Hauger *et al.*, Phys. Rev. Lett. **77**, 235 (1996); J. A.

Hauger *et al.*, Phys. Rev. C **57**, 764 (1998).
[7] P. M. Milazzo *et al.*, Phys. Rev. C **58**, 953 (1998).
[8] P. F. Mastinu *et al.*, Phys. Rev. Lett. **76**, 2646 (1996); L. Phair *et al.*, *ibid.* **79**, 3538 (1997).
[9] Y. G. Ma *et al.*, Phys. Lett. B **390**, 41 (1997).
[10] I. Iori *et al.*, Nucl. Instrum. Methods Phys. Res. A **325**, 458 (1993).
[11] R. T. de Souza *et al.*, Nucl. Instrum. Methods Phys. Res. A **295**, 109 (1990).
[12] C. Cavata *et al.*, Phys. Rev. C **42**, 1760 (1990).
[13] S. Albergo *et al.*, Nuovo Cimento **89**, 1 (1985).
[14] N. Marie *et al.*, Phys. Rev. C **58**, 256 (1998).
[15] M. B. Tsang *et al.*, Phys. Rev. Lett. **78**, 3836 (1997).
[16] D. J. Morrissey *et al.*, Annu. Rev. Nucl. Part. Sci. **44**, 27 (1994).
[17] W. Bauer, Phys. Rev. C **51**, 803 (1997).
[18] T. K. Nayak *et al.*, Phys. Rev. C **45**, 132 (1992); F. Zhu *et al.*, *ibid.* **52**, 784 (1995).
[19] H. Xi *et al.*, NSCL-MSU Report No. 1055, 1997 (unpublished); H. Xi *et al.*, Phys. Lett. B **431**, 8 (1998).
[20] H. Xi *et al.*, Phys. Rev. C **57**, R462 (1998).
[21] R. Bougault *et al.*, XXXV International Winter Meeting on Nuclear Physics, Bormio, 1997, edited by I. Iori (unpublished), p. 116.
[22] W. A. Friedman, Phys. Rev. C **42**, 667 (1990).
[23] W. G. Lynch, Annu. Rev. Nucl. Part. Sci. **37**, 493 (1987).
[24] D. R. Bowman *et al.*, Phys. Rev. C **52**, 818 (1995).
[25] P. Glassel *et al.*, Z. Phys. A **310**, 189 (1983); D. E. Fields *et al.*, Phys. Rev. Lett. **69**, 3713 (1992); G. Casini *et al.*, *ibid.* **71**, 2567 (1993); J. F. Lecolley *et al.*, Phys. Lett. B **354**, 202 (1995); L. Stuttge *et al.*, Nucl. Phys. **A539**, 511 (1992); J. Lukasic *et al.*, Phys. Rev. C **55**, 1906 (1997).
[26] V. E. Viola *et al.*, Phys. Rep. **26**, 178 (1982).
[27] M. D'Agostino *et al.*, Phys. Lett. B **371**, 175 (1996).